Superlattices and Microstructures 113 (2018) 328–336

Contents lists available at ScienceDirect

Superlattices and Microstructures

journal homepage: www.elsevier.com/locate/superlattices

Modification of back electrode with WO_3 layer and its effect on $Cu_2ZnSn(S,Se)_4$-based solar cells

Kun Shi [a], Bin Yao [a, b, **], Yongfeng Li [a, b, *], Zhanhui Ding [a], Rui Deng [c], Yingrui Sui [d], Zhenzhong Zhang [e], Haifeng Zhao [e], Ligong Zhang [e]

[a] State Key Lab of Superhard Material and College of Physics, Jilin University, Changchun 130012, China
[b] Key Laboratory of Physics and Technology for Advanced Batteries (Ministry of Education), College of Physics, Jilin University, Changchun 130012, China
[c] School of Materials Science and Engineering, Changchun University of Science and Technology, Changchun, 130022, China
[d] College of Physics, Jilin Normal University, Siping, 136000, China
[e] State Key Lab of Excited State Processes, Changchun Institute of Optics, Fine Mechanics and Physics, Chinese Academy of Sciences, Changchun, 130033, China

ARTICLE INFO

Article history:
Received 7 November 2017
Accepted 8 November 2017
Available online 8 November 2017

Keywords:
CZTSSe
WO_3
$MoSe_2$
Barrier layer
Solar cell
Interface

ABSTRACT

In the present work, we designed and prepared $Cu_2ZnSn(S,Se)_4$ (CZTSSe)-based solar cells with a new structure of Al/ITO/ZnO/CdS/CZTSSe/WO_3/Mo/SLG (S1-5) by depositing about 5-nm-thick WO_3 layer with monoclinic structure on the back electrode Mo/SLG of solar cells with the convention structure of Al/ITO/ZnO/CdS/CZTSSe/Mo/SLG (S2), with the aim of improving the power conversion efficiency (PCE) of CZTSSe-based solar cells. It is found that the average open circuit voltage (V_{oc}) increases from 346.7 mV of the S2 cells to 400.9 mV of the S1-5 cells, the average short circuit current density (J_{sc}) from 26.4 mA/cm^2 to 32.1 mA/cm^2 and the filling factor (FF) from 33.8 to 40.0 by addition of the WO_3 layer, which results in that the average PCE increases from 3.10% of the S2 cells to 5.14% of the S1-5 cells. The average increasing percent of the PCE is 65.8%. The increase in V_{oc}, J_{sc} and FF of the S1-5 cells compared to the S2 cells is attributed to that the WO_3 layer prevent the Se coming from Se ambient and CZTSSe to react with the Mo to form $MoSe_2$ and other second phases, which makes the shunt resistance (R_{sh}) of the S1-5 increase and the series resistance (R_s) and reverse saturation current density (J_0) decrease compared to the S2 cells. The decreased J_0 is main factor of improvement of the PCE. A mechanism of influence of the R_{sh}, R_s and J_0 on the PCE is also revealed. Our result demonstrates that addition of the WO_3 layer with a reasonable thickness can be a promising technical route of improving the PCE of the CZTSSe-based solar cell.

© 2017 Elsevier Ltd. All rights reserved.

1. Introduction

In the recent years, the role of thin-film solar cells becomes increasingly important in the photovoltaic field with the development of photovoltaic technology, especially Cu(In, Ga)Se_2 (CIGS) and CdTe solar cells [1,2]. However, the

* Corresponding author. Key Laboratory of Physics and Technology for Advanced Batteries (Ministry of Education), College of Physics, Jilin University, Changchun 130012, China.
** Corresponding author. State Key Lab of Superhard Material and College of Physics, Jilin University, Changchun 130012, China.
E-mail addresses: binyao@jlu.edu.cn (B. Yao), liyongfeng@jlu.edu.cn (Y. Li).

https://doi.org/10.1016/j.spmi.2017.11.013
0749-6036/© 2017 Elsevier Ltd. All rights reserved.

CIGS solar cells can hardly be applied into the reality on a large scale in the future due to the rare and high cost of indium. The cadmium in CdTe solar cells is a toxic element, which is a potential risk for environment. To solve these issues, the earth-abundant absorber material, $Cu_2ZnSn(S, Se)_4$, has received more and more attention recently as an alternative absorber for solar cells due to its suitable characteristics such as a high absorption coefficient of 10^4 ~ 10^5 cm^{-1} and band gap tenability between 1.0 and 1.5 eV [3,4]. Up to now, the highest power conversion efficiency (PCE) of CZTSSe solar cells ever reported is 12.6% [5]. However, the PCE has not been improved further since 2014. There are several factors impeding the efficiency further improvement for CZTSSe solar cells, one of them is that the back electrode Mo reacts with Se to form $MoSe_2$ and secondary phases during selenization process [6,7]. It has been reported that the over-thick $MoSe_2$ will reduce the thickness of Mo layer dramatically and deteriorate the electrical contact of CZTSSe to Mo substrate, both of which will increase the series resistance of the device significantly [8,9]. While the formation of the second phases may decrease shunt resistant (R_{sh}) and increase recombination rate. So, a lot of work has been done to avoid the formation of $MoSe_2$ by adding a barrier layer between the back contact and the absorber, such as TiN [10,11], TiB_2 [12] and Ag [13]. The barrier layer, like TiN or TiB_2, can indeed decrease the formation of $MoSe_2$, while those attempts will increase the series resistance. Although the Ag barrier can both reduce the thickness of $MoSe_2$ and the series resistance of solar cells, it is too expensive to be used as an ideal barrier for production-scale application in the future [13,14].

In this work, the formation of $MoSe_2$ is decreased successfully by inserting a WO_3 intermediate layer between back electrode and CZTSSe absorber of CZTSSe-based solar cell with the conventional structure. The open circuit voltage (V_{oc}), short circuit current density (J_{sc}) and fill factor (FF) of CZTSSe-based solar cells are increased, accordingly, the PCE is improved significantly by restraining the formation of the $MoSe_2$. The influencing mechanism of the WO_3 on the PCE is elucidated by analyzing the effect of WO_3 on the shunt resistance (R_{sh}), series resistance (R_s), ideality factor (A) and reverse saturation current (J_0).

2. Experimental details

2.1. Preparation of WO_3 thin film

The WO_3 thin films were deposited on soda-lime glass (SLG) substrate by sputtering a metal W target using a DC magnetron sputtering. The chamber was evacuated to 8×10^{-4} Pa before deposition process. The mixture of oxygen and argon flow with 28 sccm was used as the working gas. The partial pressure ratio of oxygen to argon is 3:1. During the sputtering process, the working pressure and sputtering power were 0.2 Pa and 100 W, respectively. The sputtering process lasted for 5 min to obtain a WO_3 film with a thickness of 100 nm. In order to improve the crystal quality of WO_3 and study the influence of selenization on the structure of WO_3, the as-deposited WO_3 films were firstly annealed at 400 °C for 3 h in air with a heating rate of 5 °C/min (denoted as H0), and then annealed at 550 °C for 3 h in air (denoted as H1) or for 15 min in a selenium atmosphere (denoted as H2) with a heating rate of 60 °C/min.

2.2. Device fabrication

In order to study the effect of WO_3 layer deposited upon the back electrode on the performance of CZTSSe-based solar cells, two kinds of CZTSSe-based solar cells with structures of Al/ITO/ZnO/CdS/CZTSSe/WO_3/Mo/SLG (denoted as S1) and Al/ITO/ZnO/CdS/CZTSSe/Mo/SLG (denoted as S2) were fabricated, respectively. For the S1 cell, the WO_3 layer with 5 nm (S1-5), 20 nm (S1-20) and 50 nm (S1-50) in thickness were grown on the Mo coated soda-lime glass (Mo/SLG) substrate firstly by RF magnetron sputtering with the working pressure of 0.1Pa, power of 50 W and mixed gas of oxygen and argon with the partial pressure ratio of oxygen to argon of 3:1, then the absorption layer of CZTS was deposited upon the WO_3 layer by sol-gel method followed by selenization, a CdS layer with the thickness of 60 nm was grown on CZTSSe layer by chemical bath deposition and finally, the window layers consisting of i-ZnO (50 nm) and ITO (250 nm) were sputtered on the top of the CdS layer, followed by thermal evaporation of the Al grid electrode on the top of the ITO layer. An active area of 0.19 cm^2 was defined by mechanical scribing for all solar cells. The detailed process can be found in our previous work [15,16].

2.3. Characterization

The crystal structures of the films were characterized by an X-ray diffractometer (XRD) with Cu Kα radiation ($\lambda = 1.5406$ Å). The scanning electron microscope (SEM) and compositions measurements were performed using a Hitachi S-4800 equipped with an energy-dispersive X-ray spectroscopy (EDS) system (EDAX Genesis 2000). For the power conversion efficiency measurements of CZTSSe-based solar cells, the current density–voltage curves were measured with a Keithley 2400 source meter and a solar simulator (Abet Sun 2000; AM 1.5) by a homemade probe station. The light intensity was calibrated to 100 mW/cm^2 using a Newport optical power meter (model 842-PE) certified by Newport.

3. Results and discussion

3.1. Performance and characterization of WO_3 layers

Fig. 1(a) shows the XRD pattern of WO_3 film annealed at 400 °C in air (H0). All diffraction peaks are attributed to the diffractions of WO_3 with a monoclinic structure [17], and no secondary phase is observed. In order to further improve the crystal quality of WO_3, the 400 °C annealed WO_3 films were annealed again at 550 °C for 3 h in air (H1) and for 15 min in a Se atmosphere (H2), respectively. Fig. 1(b) and (c) shows the XRD patterns of the H1 and H2, respectively. Besides the diffraction peaks of WO_3, a series of diffraction peaks related to $Na_2W_3O_{10}$ [18] are observed for H1 and H2. The peak intensity of $Na_2W_3O_{10}$ for H2 is larger than that for H1. The formation of $Na_2W_3O_{10}$ can be attributed to the reaction between Na and WO_3, which can take place as the temperature is higher than 510 °C [18]. The Na comes from the SLG substrate. The sharp increase in the intensities of the peaks of $Na_2W_3O_{10}$ implies that Na^+ can diffuse more easily from the substrate into the film as the selenium vapor exists during the annealing process. It is found that the XRD pattern of WO_3 in Fig. 1(a) is almost the same as that in Fig. 1(b), but somewhat different from that in Fig. 1(c). The three XRD peaks of WO_3 in the diffraction angle ranging from 22° to 25° is not overlapped but discrete and the full-width at half maximum of the diffraction peaks of WO_3 is also smaller than that in Fig. 1(a) and (b). These results indicate that the crystal quality of WO_3 in H2 is better than that of H1 or H0.

Fig. 2(a) and (b) show the SEM images of H1 and H2 films, respectively. It is found from Fig. 2(a) that the surface of H1 consists of two kinds of grains with several nanometers in size, one is bright and the other is dark. Moreover, the amount of bright grains is less than that of dark grains. Based on the results obtained from Fig. 1 (b), it can be deduced that the bright grains may be $Na_2W_3O_{10}$ and the dark grains may be WO_3. The nanostructured H1 is not favorable to obstruct Se diffusion due to the existence of many grain boundaries. However, the surface of H2 is smooth and consists of many micrometer scale grains, as shown in Fig. 2(b). The big grains are beneficial to depress the diffusion of selenium into the molybdenum layer to form $MoSe_2$ in the process of selenization, and the smooth surface is favorable to make the CZTSSe absorption layer grown more smoothly.

In order to figure out the electrical properties of H0, H1 and H2 films, Hall measurement was performed for the three films, as listed in Table 1. It can be seen from Table 1 that the H0 is high resistant and that the H1 and H2 behave semiconducting properties. Since WO_3 is a high resistant material with the resistivity of $2.6 \times 10^3\ \Omega\cdot$cm, the semiconducting properties of H1 and H2 should mainly come from the contribution of $Na_2W_3O_{10}$. Compared with H1, the resistivity of H2 reduced by two orders of magnitude, which may be due to the increase in crystal quality and grain size. Obviously, the H2 is more beneficial to be used as the obstruction or passivation layer in solar cell, because small resistance can result in small series resistance.

3.2. The effect of WO_3 layer on the performance of solar cell

The corresponding performance parameters of the S1 and S2 are listed in Table 2. It can be seen that the PCE of S1 decreases as the thickness of WO_3 layer increases. The PCE of S1-20 is lower than that of S1-5 is mainly because of the decline of J_{sc}, which is derived from the increase of R_s/R_{sh}. Although the V_{oc} of S1-50 is higher than that of S2, the PCE is lower for S1-50

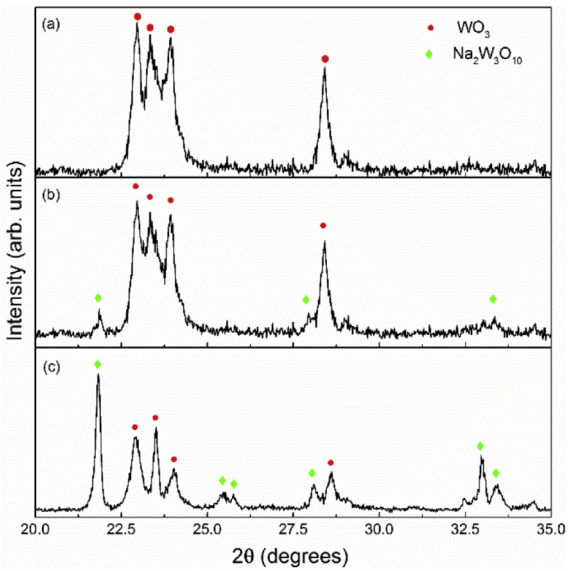

Fig. 1. XRD pattern of the (a) WO_3 film annealed at 400 °C in air (H0), (b) H0 film annealed at 550 °C for 3 h in air (H1) and (c) for 15 min in a selenium ambient (H2), respectively.

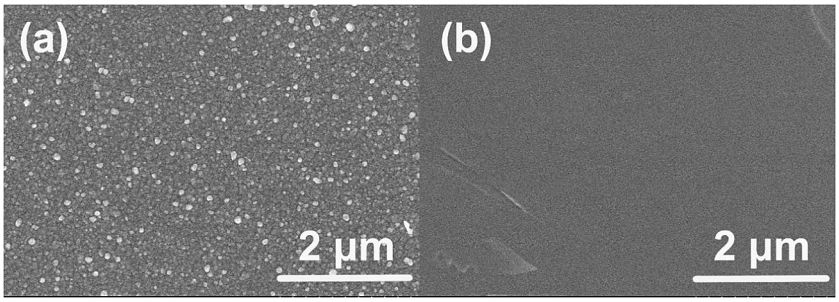

Fig. 2. Surface morphology SEM images of the H1and H2.

Table 1
Resistivity, conduction type, carrier concentration and mobility of H0, H1 and H2.

Sample	Resistivity(Ω·cm)	Type	Hall Mobility($cm^2/V·s$)	Carrier Density (cm^{-3})
H0	2.6×10^3	n	6.6×10^1	3.9×10^{13}
H1	1.1×10^1	n	8.2×10^{-1}	7.2×10^{17}
H2	2.3×10^{-1}	n	9.4×10^{-2}	2.9×10^{20}

Table 2
Performance and electrical parameters of the CZTSSe-based solar cells with (S1) and without (S2) WO_3 layer under AM 1.5G Illumination.

Samples	V_{oc} (mV)	J_{sc}(mA/cm^2)	FF (%)	PCE (%)	R_{sh}(Ω·cm^2)	R_s (Ω·cm^2)	R_s/R_{sh}	A	J_0 (mA/cm^2)
S1-5	401	34.6	39.5	5.49	334.4	2.83	0.008	1.86	0.0082
S1-20	405	22.8	40.3	3.73	167.1	2.32	0.014	2.51	0.041
S1-50	371	18.3	35.7	2.42	151.6	3.88	0.026	2.7	0.091
S2	349	28.3	33.8	3.34	144.8	4.3	0.029	2.07	0.043

due to its much lower J_{sc} than that of S2. Thus, it can be concluded that an over-thick WO_3 layer will lead to a higher internal resistance of the solar cell, which is against the promotion of PCE. The ideality factors (A) of S1-20 and S1-50 are both much higher than 2, which indicates that the recombination at the back-contact interface increases due to the over-thick WO_3 layer. Therefore, the optimal thickness of WO_3 layer for the CZTSSe-based solar cell is 5 nm based on our results.

In order to investigate the effect of WO_3 layer on the performance of solar cells, we prepared six CZTSSe-based solar cells with the structure of Al/ITO/ZnO/CdS/CZTSSe/WO_3/Mo/SLG (S1-5) and six CZTSSe-based solar cells with the structure of Al/ITO/ZnO/CdS/CZTSSe/Mo/SLG (S2) under the same technical conditions. Fig. 3 shows two typical current density (J) against voltage (V) curves obtained from the S1-5 and S2 cells, respectively. It is found that the open circuit voltage (V_{oc}), short circuit current density (J_{sc}) and fill factor (FF) of the solar cell with the WO_3 layer are larger than those of solar cells without the WO_3 layer, resulting in that the power conversion efficiency (PCE) of the S1-5 is higher than that of S2. Fig. 4 shows plots of the PCE,

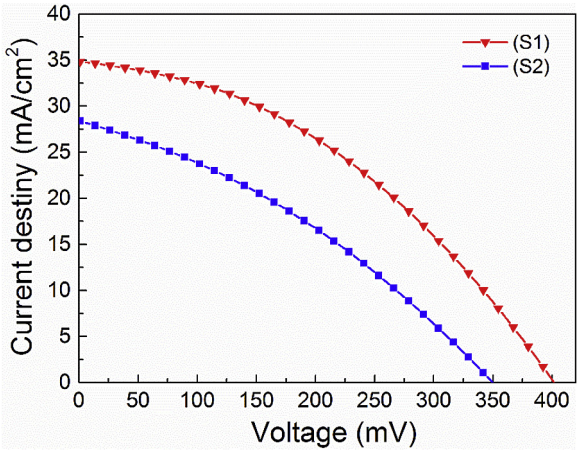

Fig. 3. Current–voltage characteristics of the CZTSSe-based solar cell with (S1-5) and without (S2) WO_3 layer under AM 1.5G illumination.

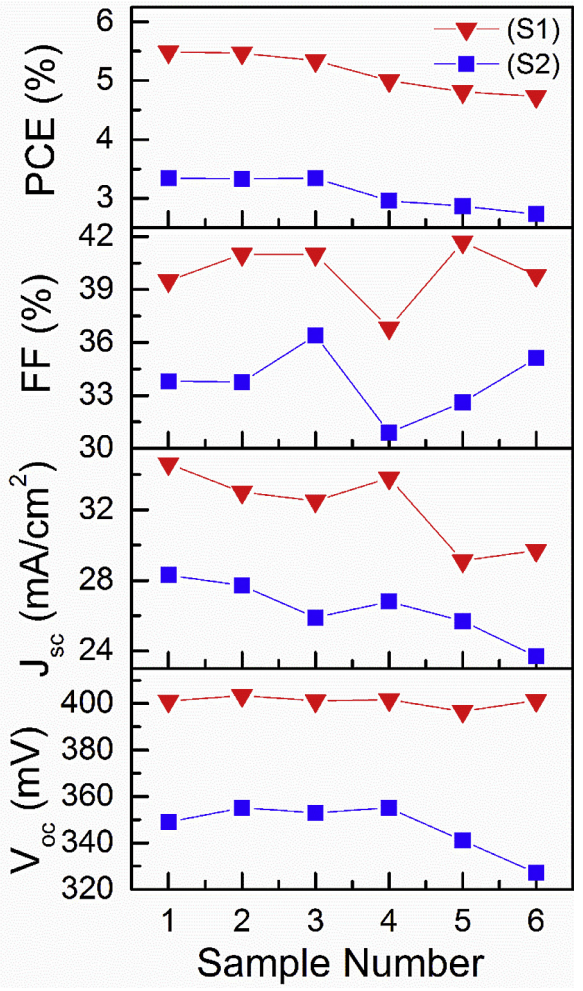

Fig. 4. Plots of the V_{oc}, J_{sc}, FF and PCE of the six CZTSSe-based solar cells with WO_3 (S1-5) and six cells without WO_3 (S2).

V_{oc}, J_{sc} and FF of the six S1-5 and six S2, which indicate that all S1-5 cells have larger PCE, V_{oc}, J_{sc} and FF than those of the S2. This demonstrates that the larger PCE of the S1-5 cells comes from the improvement in the performance of those cells and that the addition of WO_3 layer can increase the V_{oc}, J_{sc}, FF and PCE.

Fig. 5(a)-(c) show the plots of the PCE against V_{oc}, J_{sc} and FF of the CZTSSe-based solar cells with and without WO_3 layer, respectively. It is found that the PCE increases with increasing V_{oc}, J_{sc} and FF. The increase is continuous in the S1-5 or S2 cells, but interrupted between the S1-5 and S2. This implies that the difference in PCE between S1-5 and S2 cells does not come from the preparation process but the structure of the solar cells.

In order to illuminate the influence mechanism of WO_3 on the performance of CZTSSe-based solar cells, electrical parameters of the S1-5 and S2, including shunt resistance (R_{sh}), series resistance (R_s), ideality factor (A) and reverse saturation current (J_0), were calculated by using sites' method [19], as shown in Fig. 6. It can be seen that the S1-5 have higher R_{sh} but lower R_s and J_0 than that of S2. Based on V_{oc} equation of solar cell:

$$1/R_{sh}V_{oc} = J_{sc} - J_0\left(e^{\frac{qV_{oc}}{AkT}} - 1\right) \tag{1}$$

where k and T are Boltzmann constant and kelvin temperature, respectively, the higher R_{sh} and lower J_0 will lead to the increase in V_{oc}. Therefore, it can be concluded that the increase in V_{oc} of the S1-5 solar cells is ascribed to the increase of R_{sh} and the decrease of J_0 compared to the S2 solar cells, as shown in Fig. 7(a) and (b). By solving Equation (1) and combining with the R_{sh}, J_0 and A given in Fig. 7, it is deduced that the V_{oc} is mainly affected by the J_0.

Fig. 7(c) and (d) show plots of J_{sc} with R_s/R_{sh} and J_0, respectively, which reflects that the J_{sc} decreases with increasing R_s/R_{sh} and J_0, and that the J_{sc} of all the S1-5 cells is larger than that of S2 cells. Based on J_{sc} equation of solar cell:

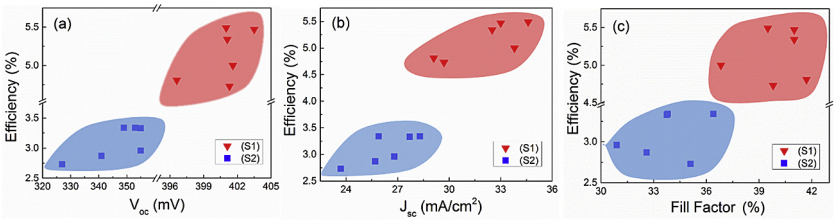

Fig. 5. Plots of the PCE vs V_{oc}(a), J_{sc}(b) and FF(c) of the six S1-5 and six S2 solar cells.

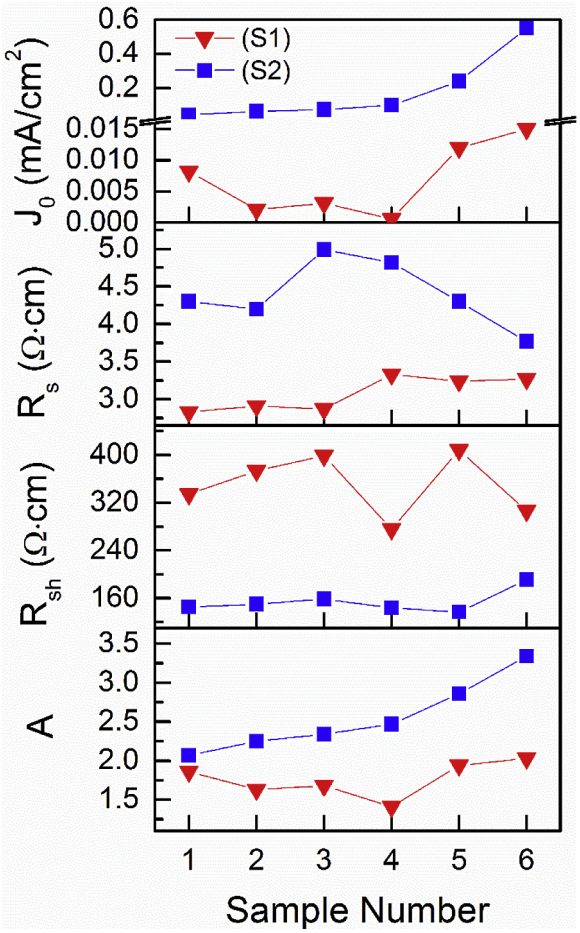

Fig. 6. R_{sh}, R_s, A and J_0 of the CZTSSe-based solar cells with(S1-5) and without WO_3 layers(S2).

$$(1 + R_s/R_{sh})J_{sc} = J_{ph} - J_0\left(e^{\frac{qJ_{sc}R_s}{AkT}} - 1\right) \tag{2}$$

where J_{ph} represents the photo-generated current density and is related to built-in field. J_{sc} is related to R_s, R_s/R_{sh} and J_0, and a notable negative correlation can be found between the J_{sc} and any parameter of R_s, R_s/R_{sh} and J_0. As shown in Fig. 6, the R_s and J_0 for S1-5 are smaller than those of S2, which will accordingly lead to a larger J_{sc}. The J_{sc} is mainly affected by R_s and J_0. Fig. 7(e) and (f) indicate that the increase of FF for the S1-5 is related to the decrease of R_s and the increase of R_{sh}.

It can be noted from Fig. 6 that the ideality factor A of the S1-5 varies in the range of 1.41–2.03, while the A of S2 is in the range of 2.07–3.34. Based on solar cell theory, the recombination of photo-generated carriers in the space charge region the neutral zone dominates if A is in the range of 1–2. As a matter of course, there should be other factors that resulting in the

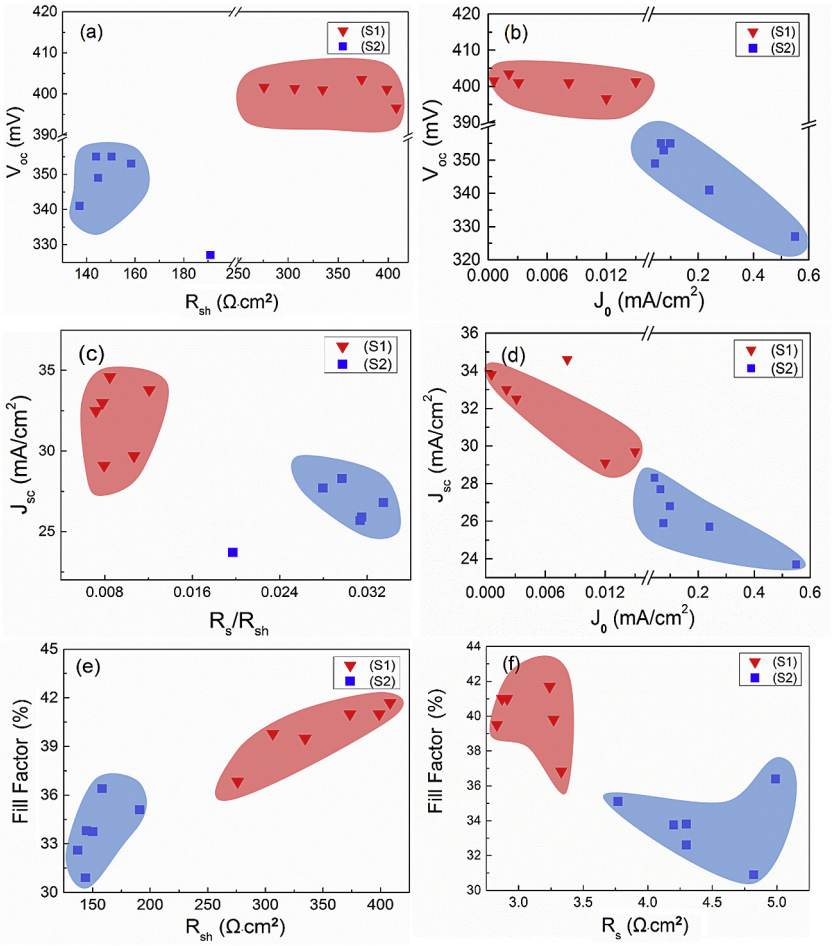

Fig. 7. Plots of V_{oc} vs R_{sh} (a) and J_0 (b), J_{sc} vs R_s/R_{sh} (c) and J_0 (d) and FF vs R_{sh} (e) and R_s (f) of the CZTSSe-based solar cells with (S1-5) and without (S2) WO_3 layer.

extra recombination of the photo-generated carriers when A is larger than 2. Considering the only change in the structures of S1-5 and S2, it is convincing that the difference in the performance of two kinds of solar cells is caused by the insertion of WO_3 layer with the thickness of 5 nm, which leads to a higher PCE of S1-5 than that of S2.

It should be noted from Fig. 7 that the J_{sc} and FF of the S1-5 and S2 cells almost vary continuously with the R_s, R_{sh} and J_0, but the V_{oc} nearly maintains a constant with the R_{sh} and J_0. Therefore, we deduce that the abrupt increase in the PCE of the S1-5 cells compared to the S2 cells shown in Fig. 5 is mainly origin from the sharply increase of V_{oc} which was caused by the decrease of J_0.

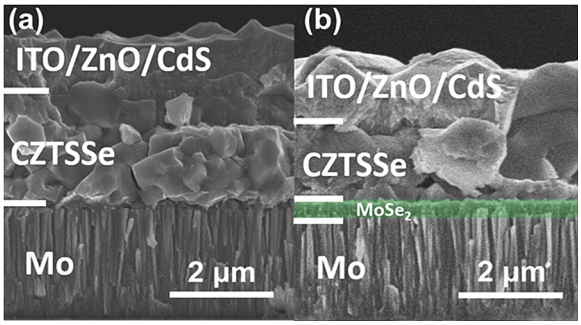

Fig. 8. Cross-sectional morphology SEM images of CZTSe solar cells. (a)-with and (b)-without WO_3 layer.

Fig. 8(a) and (b) show the cross-sectional SEM images of S1-5 and S2, respectively. As shown in Fig. 8(b), a $MoSe_2$ layer is observed as expected between the CZTSSe and Mo layers for S2. However, the $MoSe_2$ layer disappears for S1-5 with a WO_3 layer deposited at the top of Mo layer, as shown in Fig. 8(a). These results indicate that the WO_3 layer in the S1-5 cell can prevent the Se from the Se vapor or the CZTSSe layer to react with Mo. Since the 5-nm WO_3 layer is too thin, no WO_3 layer is observed at the CZTSSe/Mo interface. If no WO_3 layer is inserted between the CZTSSe and Mo layers, a $MoSe_2$ layer will come out due to the diffusion of Se into the Mo layer or a small amount of other secondary phases such as $Cu_2(S,Se)$, Zn(S,Se) and Sn(S,Se) would be formed at the interface of CZTSSe and Mo, the reaction equation can be expressed as follow [7].

$$2Cu_2ZnSn(S,Se)_4+Mo \rightarrow 2Cu_2(S,Se)+2Zn(S,Se) + 2Sn(S,Se) + Mo(S,Se)_2$$

The $MoSe_2$ layer will lead to a higher series resistance [20], and the other secondary phases will lead to a lower shunt resistance and higher recombination rate (or higher reverse saturation current density).

4. Conclusion

The CZTSSe-based solar cells with a new structure of Al/ITO/ZnO/CdS/CZTSSe/WO_3/Mo/SLG (S1-5) were prepared by depositing a WO_3 layer (~5 nm) with monoclinic structure on the back electrode Mo/SLG of solar cells with a conventional structure of Al/ITO/ZnO/CdS/CZTSSe/Mo/SLG (S2). It is found that the average V_{oc} increases from 346.7 mV for the S2 cells to 400.9 mV for the S1-5 cells, the average J_{sc} from 26.4 mA/cm^2 to 32.1 mA/cm^2 and the FF from 33.8 to 40.0 by adding a WO_3 layer, which results in an increase of the average PCE from 3.10 for the S2 cells to 5.14 for the S1-5 cells. The increased percentage of the PCE is up to 65.8%. The increase in V_{oc}, J_{sc} and FF of the S1-5 cells compared to the S2 cells is attributed to that the WO_3 layer prevents the Se from the Se vapor or the CZTSSe layer to react with the Mo to form $MoSe_2$ and the other secondary phases, which leads to the increase of the R_{sh} and the decrease of R_s for S1-5 compared to the S2 cells. The decline of J_0 is main factor that improves the PCE of the solar cells.

Acknowledgments

This work is supported by the National Natural Science Foundation of China under Grant Nos. 61774075, 11274135, and 61505067, The Science and Technology Development Project of Jilin Province under grant No. 20170101142JC, Specialized Research Fund for the Doctoral Program of Higher Education under Grant No. 20130061130011, and Ph.D. Programs Foundation of Ministry of Education of China under Grant No. 20120061120011. This work was also supported by High Performance Computing Center of Jilin University, China.

References

[1] M.A. Green, K. Emery, Y. Hishikawa, W. Warta, E.D. Dunlop, Solar cell efficiency tables (version 39), Prog. Photovoltaics Res. Appl. 20 (2012) 12–20.
[2] S.G. Kumar, K.S.R.K. Rao, Physics and chemistry of CdTe/CdS thin film heterojunction photovoltaic devices: fundamental and critical aspects, Energy Environ. Sci. 7 (2014) 45–102.
[3] W. Shockley, H.J. Queisser, Detailed balance limit of efficiency of p-n junction solar cells, J. Appl. Phys. 32 (1961) 510–519.
[4] S. Bag, O. Gunawan, T. Gokmen, Y. Zhu, T.K. Todorov, D.B. Mitzi, Low band gap liquid-processed CZTSe solar cell with 10.1% efficiency, Energy & Environ. Sci. 5 (2012) 7060.
[5] Y.S. Lee, T. Gershon, O. Gunawan, T.K. Todorov, T. Gokmen, Y. Virgus, S. Guha, $Cu_2ZnSnSe_4$Thin-Film solar cells by thermal Co-evaporation with 11.6% efficiency and improved minority carrier diffusion length, Adv. Energy Mater. 5 (2015) 1401372.
[6] P. Jackson, D. Hariskos, E. Lotter, S. Paetel, R. Wuerz, R. Menner, W. Wischmann, M. Powalla, New world record efficiency for Cu(In,Ga)Se_2 thin-film solar cells beyond 20%, Prog. Photovoltaics Res. Appl. 19 (2011) 894–897.
[7] J.J. Scragg, J.T. Watjen, M. Edoff, T. Ericson, T. Kubart, C. Platzer-Bjorkman, A detrimental reaction at the molybdenum back contact in $Cu_2ZnSn(S,Se)_4$ thin-film solar cells, J. Am. Chem. Soc. 134 (2012) 19330–19333.
[8] X. Zhu, Z. Zhou, Y. Wang, L. Zhang, A. Li, F. Huang, Determining factor of $MoSe_2$ formation in Cu(In,Ga)Se_2 solar Cells, Sol. Energy Mater. Sol. Cells 101 (2012) 57–61.
[9] B. Vermang, J.T. Watjen, V. Fjallstrom, F. Rostvall, M. Edoff, R. Kotipalli, F. Henry, D. Flandre, Employing Si solar cell technology to increase efficiency of ultra-thin Cu(In,Ga)Se_2 solar cells, Prog. photovoltaics 22 (2014) 1023–1029.
[10] J.J. Scragg, T. Kubart, J.T. Wätjen, T. Ericson, M.K. Linnarsson, C. Platzer-Björkman, Effects of back contact instability on Cu_2ZnSnS_4 Devices and processes, Chem. Mater. 25 (2013) 3162–3171.
[11] B. Shin, Y. Zhu, N.A. Bojarczuk, S. Jay Chey, S. Guha, Control of an interfacial $MoSe_2$ layer in $Cu_2ZnSnSe_4$ thin film solar cells: 8.9% power conversion efficiency with a TiN diffusion barrier, Appl. Phys. Lett. 101 (2012) 053903.
[12] F. Liu, K. Sun, W. Li, C. Yan, H. Cui, L. Jiang, X. Hao, M.A. Green, Enhancing the Cu_2ZnSnS_4 solar cell efficiency by back contact modification: inserting a thin TiB_2 intermediate layer at Cu_2ZnSnS_4/Mo interface, Appl. Phys. Lett. 104 (2014) 051105.
[13] H. Cui, X. Liu, F. Liu, X. Hao, N. Song, C. Yan, Boosting Cu_2ZnSnS_4 solar cells efficiency by a thin Ag intermediate layer between absorber and back contact, Appl. Phys. Lett. 104 (2014) 041115.
[14] J. Li, Y. Zhang, W. Zhao, D. Nam, H. Cheong, L. Wu, Z. Zhou, Y. Sun, A temporary barrier effect of the alloy layer during selenization: tailoring the thickness of $MoSe_2$ for efficient $Cu_2ZnSnSe_4$ Solar cells, Adv. Energy Mater. 5 (2015) 1402178.
[15] Z.Y. Xiao, B. Yao, Y.F. Li, Z.H. Ding, Z.M. Gao, H.F. Zhao, L.G. Zhang, Z.Z. Zhang, Y.R. Sui, G. Wang, Influencing mechanism of the selenization temperature and time on the power conversion efficiency of $Cu_2ZnSn(S,Se)_4$-Based solar cells, ACS Appl. Mater. interfaces 8 (2016) 17334–17342.
[16] Z.-Y. Xiao, Y.-F. Li, B. Yao, Z.-H. Ding, R. Deng, H.-F. Zhao, L.-G. Zhang, Z.-Z. Zhang, Significantly enhancing the stability of a Cu_2ZnSnS_4 aqueous/ethanol-based precursor solution and its application in $Cu_2ZnSn(S,Se)_4$ solar cells, RSC Adv. 5 (2015) 103451–103457.
[17] R. Diehl, G. Brandt, E. Salje, The crystal structure of triclinic WO_3, Acta Crystallogr. Sect. B Struct. Crystallogr. Cryst. Chem. 34 (1978) 1105–1111.

[18] S. Chatterjee, P.K. Mahapatra, A.K. Singh, R.N.P. Choudhary, Structural, electrical and dielectric properties of $Na_2W_3O_{10}$ ceramic, Mater. Lett. 57 (2003) 2616–2620.
[19] See http://opvap.com/jsc.php.
[20] C.-J. Hsu, H.-S. Duan, W. Yang, H. Zhou, Y. Yang, Benign solutions and innovative sequential annealing processes for high performance $Cu_2ZnSn(Se,S)_4$ Photovoltaics, Adv. Energy Mater. 4 (2014) 1301287.